Science
AAAS

Response to Comments on "Large Volcanic Aerosol Load in the Stratosphere Linked to Asian Monsoon Transport"

Adam E. Bourassa *et al.*

Science **339**, 647 (2013);
DOI: 10.1126/science.1227961

Response to Comments on "Large Volcanic Aerosol Load in the Stratosphere Linked to Asian Monsoon Transport"

Adam E. Bourassa,[1]* Alan Robock,[2] William J. Randel,[3] Terry Deshler,[4] Landon A. Rieger,[1] Nicholas D. Lloyd,[1] E. J. Llewellyn,[1] Douglas A. Degenstein[1]

Fromm *et al*. and Vernier *et al*. suggest that their analyses of satellite measurements indicate that the main part of the Nabro volcanic plume from the eruption on 13 June 2011 was directly injected into the stratosphere. We address these analyses and, in addition, show that both wind trajectories and height-resolved profiles of sulfur dioxide indicate that although the eruption column may have extended higher than the Smithsonian report we highlighted, it was overwhelmingly tropospheric. Additionally, the height-resolved sulfur dioxide profiles provide further convincing evidence for convective transport of volcanic gas to the stratosphere from deep convection associated with the Asian monsoon.

The initial altitude of the Nabro eruption and the location of the tropopause are important factors in this study (*1*). We used the Cloud Aerosol Lidar and Infrared Pathfinder Satellite Observation satellite (CALIPSO) overpass on 16 June, which was the closest in time and space to the Nabro eruption, to corroborate the aviation advisory report of an eruption altitude extending from 9 to 14 km. Unfortunately, CALIPSO measurements, which would certainly be the best tool for locating the plume altitude, are not available during 13 to 14 June. Fromm *et al*. (*2*) have used a combination of nadir imagery and Microwave Limb Sounder (MLS) vertical profiles of SO_2 to suggest an eruption confined to stratospheric altitudes that "fully explains" the observed stratospheric aerosol load and distribution without any interaction with the Asian monsoon anticyclone. Vernier *et al*. (*3*) have used CALIPSO measurements from several days after, and large distances from, the eruption to suggest direct injection into the stratosphere. Neither Fromm *et al*. nor Vernier *et al*. address two key aspects of our analysis. These are (i) the observed transport and interaction of the SO_2 plume with the Asian monsoon anticyclone, which, as will be shown here, is only consistent with tropospheric winds, and (ii) the Optical Spectrograph and Infra-Red Imaging System (OSIRIS) measurements of the resulting stratospheric aerosol enhancements extending up to 21 km and collocated with the anticyclone (*1*). In addition, analysis of the MLS SO_2 measurements presented here provides further evidence for lofting of tropospheric SO_2 to the stratosphere through convective processes associated with the monsoon circulation.

[1]Institute of Space and Atmospheric Studies, University of Saskatchewan, Saskatchewan, SK S7N 5E2, Canada. [2]Department of Environmental Sciences, Rutgers University, New Brunswick, NJ 08901, USA. [3]National Center for Atmospheric Research, Boulder, CO 80307, USA. [4]Department of Atmospheric Science, University of Wyoming, Laramie, WY 82071, USA.

*To whom correspondence should be addressed. E-mail: adam.bourassa@usask.ca

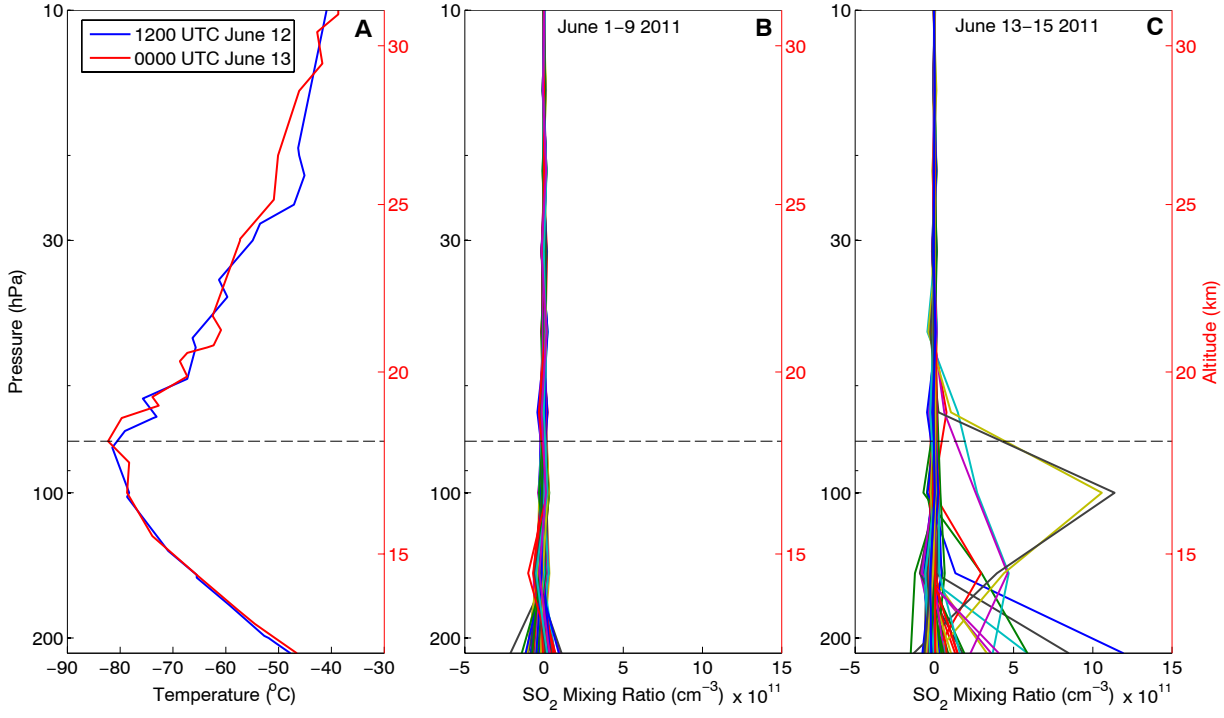

Fig. 1. **(A)** Temperature sounding from Abha, Saudi Arabia, which is the nearest location to Nabro, on 12 and 13 June 2011. The cold-point tropopause is at an altitude of 18.1 km and 78.2 hPa, which corresponds to a potential temperature of 396 K. **(B)** All of the SO_2 number density profiles measured by MLS in a 10-day period before the eruption in the geographic region of the early plume transport over northeast Africa (5° to 30°N, 14° to 45°E). **(C)** All MLS SO_2 profiles in the same geographic region during 13 to 15 June. Profiles are retrieved only at discrete pressure levels and are shown here using a linear interpolation between retrieved levels. Reported mixing ratios are converted to number densities using the Abha sounding pressure and temperatures. Each profile is shown in a distinct solid line color. The cold-point tropopause pressure from the Abha sounding is marked by the solid black line.

The cold-point tropopause, marking a sharp change in static stability and humidity, was measured at 18.1 km or 78.2 hPa at Abha, Saudi Arabia, the nearest radio sounding to Nabro, Fig. 1A. This corresponds to a potential temperature of 396 K and is typical of the tropical tropopause layer, which extends up to altitudes of 18.5 km (*4*). Figure 1 also shows all height-resolved Microwave Limb Sounder (MLS) profiles of SO_2 within 3 days of the eruption and over northeast Africa. Enhanced profiles from the volcanic plume are clear, and the overwhelming fraction of the SO_2 density occurs between 100 hPa (16 km) and 200 hPa (13 km), which is below the cold-point tropopause.

This tropopause altitude corresponds to a sharp shear in the National Centers for Environmental Prediction reanalysis wind fields. Tropospheric wind fields at 13- and 16-km altitude (1) are consistent with the measured Global Ozone Monitoring Experiment-2 (GOME-2) SO_2 plume transport toward and within the anticyclone (1), whereas stratospheric winds are ubiquitously easterly. Forward trajectories from the Nabro eruption at upper tropospheric and lower stratospheric altitudes are shown in Fig. 2. Only trajectories starting below 17 km, which are below the tropopause, are consistent with the measured SO_2 plume evolution. Trajectories at 17.5 km and above travel almost straight west and are not consistent with the SO_2 plume evolution.

Fromm *et al*. use MLS data to suggest a stratospheric plume of SO_2 from the Nabro eruption through mid-latitude Asia. They use "stratospheric enhancement" criteria that require either an SO_2 enhancement at both 100 hPa and 68 hPa or an SO_2 enhancement at 100 hPa above 380 K potential temperature. Figure 3 shows a similar analysis; however, we have relaxed these criteria and show any point where the SO_2 rises above 15 parts per billion by volume (ppbv) at 68 hPa or 30 ppbv at 100 hPa. These correspond to the lowest levels of SO_2 that result in essentially no detections during the pre-eruption period 1 to 12 June. Successive panels of Fig. 3 show the time evolution of MLS detections along with forward trajectories from Nabro and corresponding GOME-2 SO_2 column density. The analysis of Fromm *et al*. does not reveal the progression of the 100 hPa SO_2 along the east and south edges of the anticyclone due to their 380 K criterion, which neglects these points due to the natural falling of isentropes with latitude. This plume path is consistent with both column SO_2 evolution and trajectories initialized at tropospheric altitudes of 15 to 16 km.

A very interesting feature of this analysis is the appearance of many stratospheric SO_2 enhancements at 68 hPa after 18 June along the southeast edge of the anticyclone, the region associated with deep convective activity (*5*). These points, which are not associated with coincident enhancements at 100 hPa and cannot be explained by trajectories from Nabro, provide further convincing evidence for convective lofting of the volcanic plume. The five contiguous SO_2 enhancements at 68 hPa just northwest of Nabro on 14 June are associated with coincident or nearby large tropospheric (100 hPa) enhancements and may be the result of the relatively coarse MLS averaging kernel. Enhancements at this level are essentially not observed again until the lower-level plume reaches the southeast side of the monsoon.

During the Asian monsoon season, the tropopause remains cold and high, at ~17.0 to 17.4 km, over the entire anticyclone region, and does not decrease until north of 40°N (*6*). The layer detected by CALIPSO at 15 to 17 km and 43°N shown by Vernier *et al*. in their figure 1 is below this climatological cold point and is consistent in time and location with trajectories with initial altitudes between 16 and 17 km. For purely isentropic transport, the 390 K potential temperature of the layer places it below the 396 K cold-point tropopause measured near Nabro. The CALIPSO browse imagery for several days after the eruption shows two layers of low-depolarization backscatter in many of the measurements collocated with the SO_2 plume, often a thin layer in the upper troposphere near 16 km and a second layer typically extending over 10 to 14 km. The GOME-2 SO_2 measurements also show two distinct paths from Nabro toward the monsoon. These are slightly separated in latitude and correspond to two altitude layers likely separated during transport by wind shear. Trajectory analysis shows that the higher-altitude layer traveled slower than the lower-altitude layer, suggesting that the latter was responsible for the large region of high SO_2 density already observed on the eastern side of the anticyclone on 16 June. In fact, the CALIPSO transect shown by Vernier *et al*. in Fig. 1B is one example of the measurements that show the lower-altitude path of SO_2 and aerosol from Nabro to

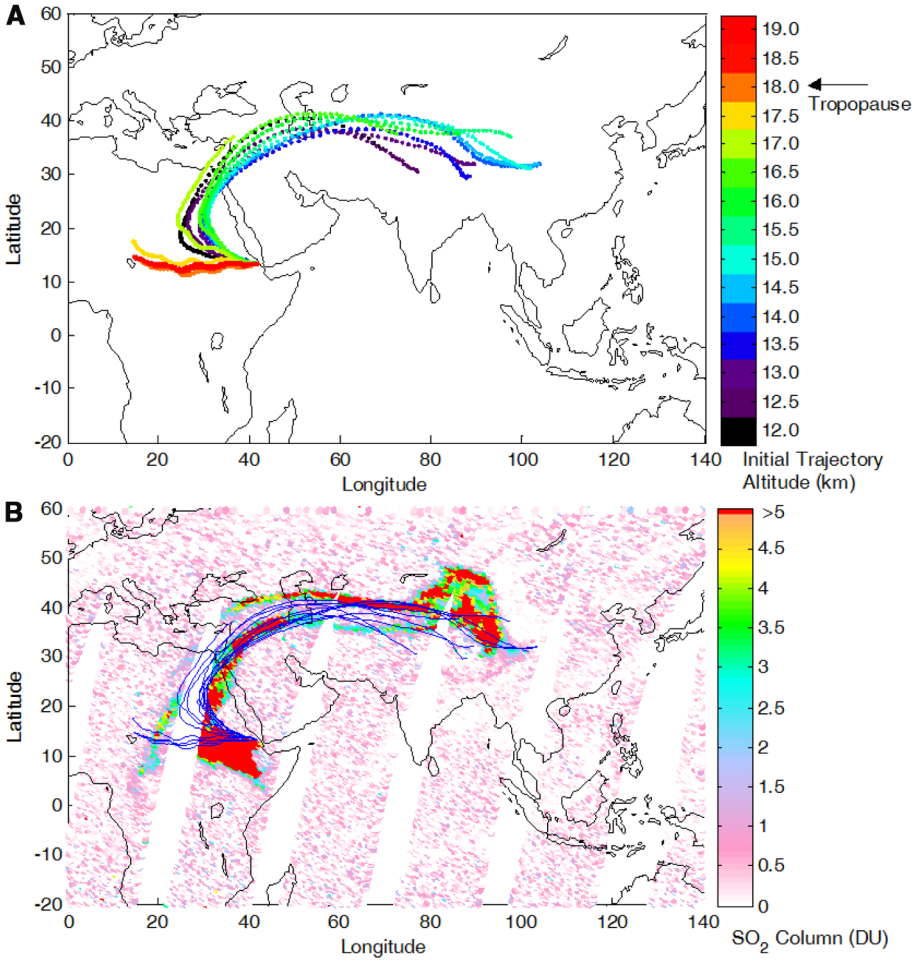

Fig. 2. (**A**) Forward trajectories from Nabro starting at 0000 UTC 13 June and running for 96 hours, i.e., until the end of 16 June. Only trajectories starting below 17 km, at least 1 km below the tropopause, are consistent with the SO_2 plume evolution measured by GOME-2 on 16 June shown in (**B**) with the trajectories overlaid in blue. Trajectories between 13 and 15 km are most consistent with the large and fast-moving SO_2 plume on the leading edge of the eruption that caused the large region of high-density SO_2 observed on the eastern side of the monsoon on 16 June. Trajectories initialized at and above 17.5 km track consistently west. All trajectory calculations were performed using the Hybrid Single Particle Lagrangian Integrated Trajectory (HYSPLIT) model.

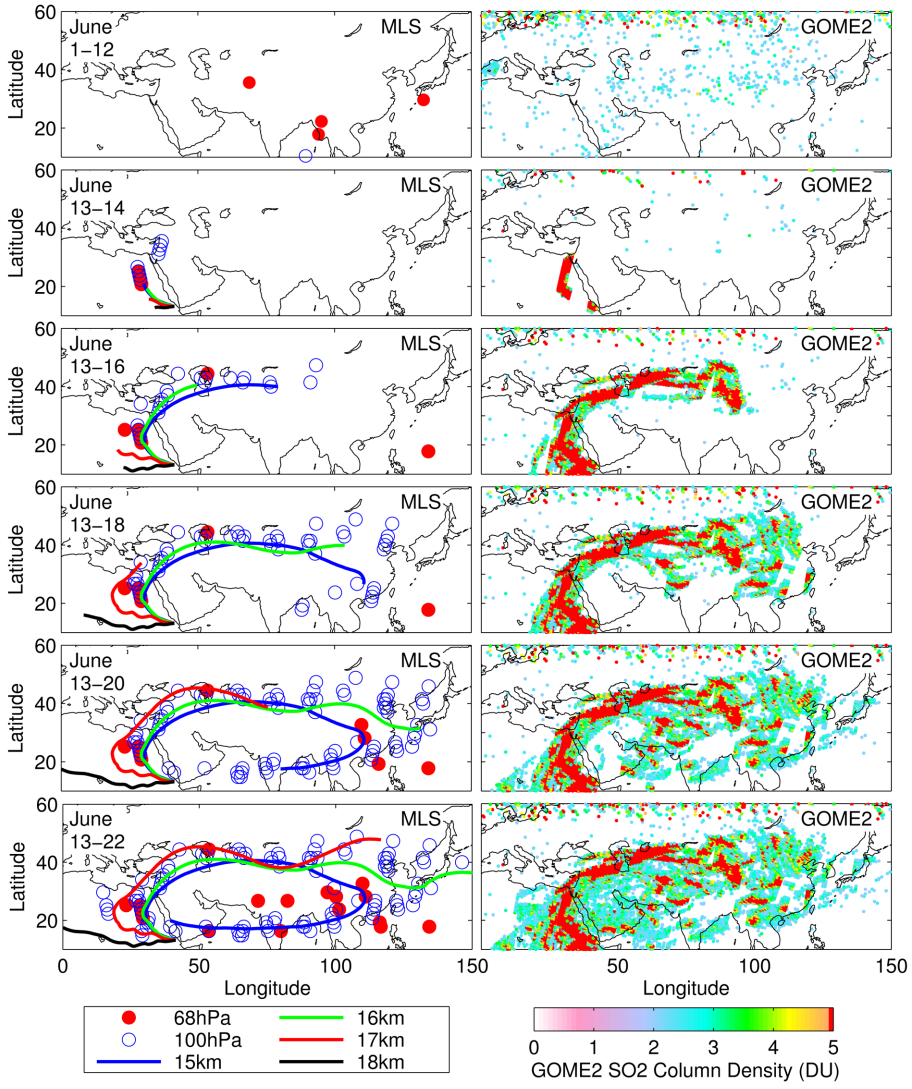

Fig. 3. The time evolution of MLS and GOME-2 SO_2 measurements. (Left) MLS SO_2 detections at 100 hPa and 68 hPa pressure levels, along with forward trajectories from Nabro. (Right) GOME-2 total column SO_2. Each panel after 13 June shows all the measurements from 13 June to the indicated date.

the monsoon region with a low-depolarization scattering layer at 11 to 12 km and 37°N. It appears weaker than the 15- to 17-km layer because the majority of this plume is already much farther east. The preceding CALIPSO orbit intersects the region of high SO_2 density on the eastern side and shows an extended sheared aerosol plume between 11 and 15 km.

Vernier *et al*. show the probability density of the occurrence of the highest aerosol layer with respect to the GEOS-5 tropopause for CALIPSO measurements on 15 to 20 June. However, the plume has already reached the eastern side of the anticyclone circulation on 16 June. CALIPSO aerosol observations after this time in the monsoon region could be evidence of convective transport. The entrainment and build up of the Nabro aerosol cloud by the Asian monsoon in July is captured well by OSIRIS (*1*, *5*). Analyses to determine the initial injection altitude should focus on the period 13 to 15 June and on aerosol layers coincident with the observed SO_2 plume transport to preclude nonvolcanic layers. Also, GEOS-5 tropopause heights are known to be problematic and often too low in the monsoon region (*7*).

Brightness temperature imagery is difficult to use to estimate the precise altitude and convective nature of a volcanic plume due to thermal disequilibrium. The plume can be hotter than the local atmosphere due to initially hot eruption gas temperature and can also experience substantial plume-top undercooling due to adiabatic decompression. These factors are known to cause considerable uncertainty in the plume altitude determination using this method (*8*, *9*). Nonetheless, Fromm *et al*. report that both cloud-top pressure and brightness temperature indicate a plume-top altitude of ~16 km, which is 2 km below the cold-point tropopause.

Finally, a small fraction of the total volcanic SO_2 directly injected into the stratosphere does not explain the resulting aerosol load. The total mass of SO_2 erupted by Nabro has been estimated at 1.3 Tg by the Ozone Monitoring Instrument and 1.5 Tg by the Infrared Atmospheric Sounding Interferometer (*10*), which is similar to Sarychev, a high-latitude stratospheric eruption, which injected a total of 1.2 Tg of SO_2 (*11*). For Nabro, Fig. 1 shows that the overwhelming fraction of the SO_2 density associated with the early plume was below the cold-point tropopause. These, along with the early aviation advisory altitudes of 9 to 14 km, and the consistency of the plume transport with tropospheric winds, clearly indicate a dominantly tropospheric eruption. Yet, the Nabro stratospheric aerosol enhancement is relatively large and is comparable to that observed after the Sarychev eruption (*1*, *6*). The appearance of stratospheric MLS SO_2 detections collocated with deep convection, and the initial stratospheric aerosol collocated with the Asian monsoon (*1*, *5*), suggest an important role for the monsoon in the resulting stratospheric aerosol load.

References and Notes

1. A. E. Bourassa *et al*., *Science* **337**, 78 (2012).
2. M. Fromm *et al*., *Science* **339**, 647 (2013); www.sciencemag.org/cgi/content/full/339/6120/647-c.
3. J.-P. Vernier *et al*., *Science* **339**, 647 (2013); www.sciencemag.org/cgi/content/full/339/6120/647-d.
4. S. Fueglistaler *et al*., *Rev. Geophys.* **47**, RG1004 (2009).
5. M. Park, W. J. Randel, A. Gettelman, S. T. Massie, J. H. Jiang, *J. Geophys. Res.* **112**, D16309 (2007).
6. W. J. Randel *et al*., *J. Geophys. Res.* **108**, 4024 (2003).
7. L. L. Pan, L. A. Munchak, *J. Geophys. Res.* **116**, D12201 (2011).
8. A. W. Woods, S. Self, *Nature* **355**, 628 (1992).
9. R. E. Holasek, S. Self, A. W. Woods, *J. Geophys. Res.* **101**, 27635 (1996).
10. L. Clarisse *et al*., *Atmos. Meas. Tech.* **5**, 581 (2012).
11. J. M. Haywood *et al*., *J. Geophys. Res.* **115**, D21212 (2010).

Acknowledgments: The authors gratefully acknowledge the the National Oceanic and Atmospheric Administration's Air Resources Laboratory for the provision of the HYSPLIT transport and dispersion model and Real-Time Environmental Applications and Display sYstem Web site (http://ready.arl.noaa.gov) used in this publication. MLS data are publically available at http://mls.jpl.nasa.gov/products/so2_product.php. Sounding data courtesy of the NOAA/ESRL Radiosonde Database. A.R. was supported by NSF grant AGS-1157525.

23 August 2012; accepted 19 November 2012
10.1126/science.1227961